University of Groningen

Measurements of the absolute branching fractions of ω- Decays and test of the Δi=1/2 rule

BESIII Collaboration; Kalantar-Nayestanaki, N.; Kavatsyuk, M.; Messchendorp, J.

Published in:
Physical Review D

DOI:
10.1103/PhysRevD.108.L091101

IMPORTANT NOTE: You are advised to consult the publisher's version (publisher's PDF) if you wish to cite from it. Please check the document version below.

Document Version
Publisher's PDF, also known as Version of record

Publication date:
2023

Link to publication in University of Groningen/UMCG research database

Citation for published version (APA):
BESIII Collaboration, Kalantar-Nayestanaki, N., Kavatsyuk, M., & Messchendorp, J. (2023). Measurements of the absolute branching fractions of ω- Decays and test of the Δi=1/2 rule. *Physical Review D*, *108*(9), Article L091101. https://doi.org/10.1103/PhysRevD.108.L091101

Copyright
Other than for strictly personal use, it is not permitted to download or to forward/distribute the text or part of it without the consent of the author(s) and/or copyright holder(s), unless the work is under an open content license (like Creative Commons).

The publication may also be distributed here under the terms of Article 25fa of the Dutch Copyright Act, indicated by the “Taverne” license. More information can be found on the University of Groningen website: https://www.rug.nl/library/open-access/self-archiving-pure/taverne-amendment.

Take-down policy
If you believe that this document breaches copyright please contact us providing details, and we will remove access to the work immediately and investigate your claim.

Downloaded from the University of Groningen/UMCG research database (Pure): http://www.rug.nl/research/portal. For technical reasons the number of authors shown on this cover page is limited to 10 maximum.

Download date: 01-02-2024

PHYSICAL REVIEW D **108,** L091101 (2023)

Letter

Measurements of the absolute branching fractions of Ω^- decays and test of the $\Delta I = 1/2$ rule

M. Ablikim *et al.*[*]
(BESIII Collaboration)

(Received 13 September 2023; accepted 11 October 2023; published 21 November 2023)

Based on a dataset of $(27.12 \pm 0.10) \times 10^8$ $\psi(3686)$ events collected at the BESIII experiment, the absolute branching fractions of the three dominant Ω^- decays are measured to be $\mathcal{B}_{\Omega^- \to \Xi^0 \pi^-} = (25.03 \pm 0.44 \pm 0.53)\%$, $\mathcal{B}_{\Omega^- \to \Xi^- \pi^0} = (8.43 \pm 0.52 \pm 0.28)\%$, and $\mathcal{B}_{\Omega^- \to \Lambda K^-} = (66.3 \pm 0.8 \pm 2.0)\%$, where the first and second uncertainties are statistical and systematic, respectively. The ratio between $\mathcal{B}_{\Omega^- \to \Xi^0 \pi^-}$ and $\mathcal{B}_{\Omega^- \to \Xi^- \pi^0}$ is determined to be $2.97 \pm 0.19 \pm 0.11$, which is in good agreement with the PDG value of 2.74 ± 0.15, but greater by more than four standard deviations than the theoretical prediction of 2 obtained from the $\Delta I = 1/2$ rule.

DOI: 10.1103/PhysRevD.108.L091101

Although the Ω^- baryon was discovered 60 years ago [1], its spin was not experimentally determined until 2006 [2], under the assumption that the spin of Ξ_c^0 is $1/2$. The first model-independent determination of the Ω^- spin was conducted by the BESIII collaboration in 2021 [3], and many of its properties still remain unknown. The Ω^- baryon plays a unique role in the baryon family as the only decuplet baryon that solely decays weakly. The weak decays of the octet baryons and the decays of Ω^- provide important information about the interplay between the strong and weak interactions [4–8].

Although isospin is not conserved in weak interactions, there is an experimentally well-established $\Delta I = 1/2$ rule, which states that in weak interactions, the $\Delta I = 1/2$ amplitude is strongly enhanced, while the $\Delta I = 3/2$ amplitude is suppressed. In general, this rule is well satisfied [9–12]. For example, the $\Lambda \to p\pi^-$ and $\Lambda \to n\pi^0$ branching fractions (BFs) [13] imply that the $\Delta I = 3/2$ amplitude in Λ decays is less than 2% [14]. The only significant violation of the $\Delta I = 1/2$ rule is observed in Ω^- decays. The BFs of the three dominant decays of Ω^- listed by the Particle Data Group (PDG) [13] were measured by the CERN-WA-046 experiment nearly 40 years ago [15]. Using the 40-year-old data, the ratio between the BFs of $\Omega^- \to \Xi^0\pi^-$ and $\Omega^- \to \Xi^-\pi^0$ ($\mathcal{B}_{\Omega^- \to \Xi^0 \pi^-}/\mathcal{B}_{\Omega^- \to \Xi^- \pi^0}$) is 2.74 ± 0.15 [13], while the value predicted by the $\Delta I = 1/2$ rule is 2 [5,16]. These results have never been confirmed by any other experiment, leading to some skepticism [6,10,12]. There are two points of view: one suggests abandoning the $\Delta I = 1/2$ rule, and obtaining more data to make phenomenologically reliable predictions [6]; the other assumes the $\Delta I = 1/2$ rule to be true and that new measurements will overturn the previous results [16,17]. To resolve this, new measurements of the BFs for Ω^- decays are urgently needed. With the world's largest $\psi(3686)$ data sample, BESIII has an excellent opportunity to measure the absolute BFs of Ω^- decays and test the $\Delta I = 1/2$ rule.

In this Letter, we utilize a double-tag (DT) method to measure the absolute BFs of the $\Omega^- \to \Xi^0\pi^-$, $\Omega^- \to \Xi^-\pi^0$, and $\Omega^- \to \Lambda K^-$ decays (unless otherwise noted, the charge-conjugated decays are always implied). The single-tag (ST) events of $\bar{\Omega}^+$ baryons are reconstructed via the decay $\bar{\Omega}^+ \to \bar{\Lambda} K^+$. The events where a signal candidate can be reconstructed from the particles recoiling against the ST $\bar{\Omega}^+$ baryon are called DT events. To improve the detection efficiencies, only the π^-, π^0, and K^- mesons from Ω^- decays are reconstructed on the signal side for the three Ω^- decay channels. The BF of a signal decay is determined by

$$\mathcal{B}_{\rm sig} = N_{\rm DT}\,\epsilon_{\rm ST}/(N_{\rm ST}\,\epsilon_{\rm DT}) = N_{\rm DT}/(N_{\rm ST}\,\epsilon_{\rm sig}), \qquad (1)$$

where $N_{\rm ST}$ and $N_{\rm DT}$ are the ST and DT yields, respectively. The $\epsilon_{\rm sig} = \epsilon_{\rm DT}/\epsilon_{\rm ST}$ is the signal efficiency in the presence of an ST $\bar{\Omega}^+$ baryon, where $\epsilon_{\rm ST}$ and $\epsilon_{\rm DT}$ are the ST and DT efficiencies, respectively.

The analysis is based on a sample of $(27.12 \pm 0.10) \times 10^8$ $\psi(3686)$ events [18] collected with the BESIII detector at the BEPCII collider. The BESIII detector [19] records symmetric e^+e^- collisions provided by the BEPCII storage ring [20], which operates with a peak luminosity of

---

[*] Full author list given at the end of the article.

1×10^{33} cm^{-2} s^{-1} in the center-of-mass energy range from 2.0 to 4.95 GeV. BESIII has collected large data samples in this energy region [21,22]. The cylindrical core of the BESIII detector covers 93% of the full solid angle and consists of a helium-based multilayer drift chamber (MDC), a plastic scintillator time-of-flight system (TOF), and a CsI(Tl) electromagnetic calorimeter (EMC), which are all enclosed in a superconducting solenoidal magnet providing a 1.0 T magnetic field. The solenoid is supported by an octagonal flux-return yoke with resistive plate counter muon identification modules interleaved with steel. The charged-particle momentum resolution at 1 GeV/c is 0.5%, and the dE/dx resolution is 6% for electrons from Bhabha scattering. The EMC measures photon energies with a resolution of 2.5% (5%) at 1 GeV in the barrel (end cap) region. The time resolution in the TOF barrel region is 68 ps, while that in the end cap region was 110 ps. The end cap TOF system was upgraded in 2015 using multigap resistive plate chamber technology, providing a time resolution of 60 ps, which benefits about 83% of the data used in this analysis [23–25].

Monte Carlo (MC) simulation samples are used to optimize the event selection and estimate the background. The simulation is performed by the GEANT4-based [26] BESIII software system [27], which includes the geometric description of the BESIII detector and the detector response. The simulation models the beam energy spread and initial state radiation in the e^+e^- annihilations with the generator KKMC [28]. The known decay modes of $\psi(3686)$ are modeled with EvtGen [29], and the remaining unknown decays are modeled with Lundcharm [30]. Final state radiation from charged final state particles is incorporated using PHOTOS [31]. The signal MC samples, $\Omega^- \to X$, used to determine the ST efficiency, and $\Omega^- \to \Xi^0(\to X)\pi^-$, $\Omega^- \to \Xi^-(\to X)\pi^0$, and $\Omega^- \to \Lambda(\to X)K^-$, used to determine the DT efficiency, are generated uniformly in phase space. Final state X indicates inclusive decay, and each sample consists of 2.54 million events.

We first measure the absolute BFs for the decay channels $\Omega^- \to \Xi^0\pi^-$ and $\Omega^- \to \Xi^-\pi^0$. Charged tracks detected in the MDC are required to be within a polar angle (θ) range of $|\cos\theta| < 0.93$, where θ is the polar angle with respect to the symmetry axis of the MDC. Particle identification (PID) for charged track combines measurements of the d$E/$dx in the MDC and the flight time in the TOF to form a likelihood $\mathcal{L}(h)(h = p, K, \pi)$ for each hadron h hypothesis. Charged tracks with $\mathcal{L}(p) > \mathcal{L}(K)$, $\mathcal{L}(p) > \mathcal{L}(\pi)$, and $\mathcal{L}(p) > 0.001$ are identified as protons, and those with $\mathcal{L}(K) > \mathcal{L}(\pi)$ are identified as kaons. The remaining charged tracks are assigned as pions by default.

For $\bar{\Lambda}$ candidates, the $\bar{p}\pi^+$ pairs are constrained to have a common vertex, and the invariant mass of a $\bar{p}\pi^+$ combination is required to be within $[1.111, 1.121]$ GeV$/c^2$. Vertex fits are performed to the $\bar{\Lambda}K^+$ pairs to improve the mass resolution of the $\bar{\Omega}^+$ candidates. If there is more than one $\bar{\Omega}^+$ candidate, the one with the minimum value of $\Delta E = |E_{\bar{\Omega}^+} - E_{\rm beam}|$ is kept for further analysis, where $E_{\bar{\Omega}^+}$ is the energy of the reconstructed $\bar{\Omega}^+$ candidate in the e^+e^- center-of-mass system and $E_{\rm beam}$ is the beam energy. In addition, the invariant mass of $\bar{\Lambda}K^+$ ($M_{\bar{\Lambda}K^+}$) must lie in the $\bar{\Omega}^+$ signal region of $[1.664, 1.680]$ GeV$/c^2$.

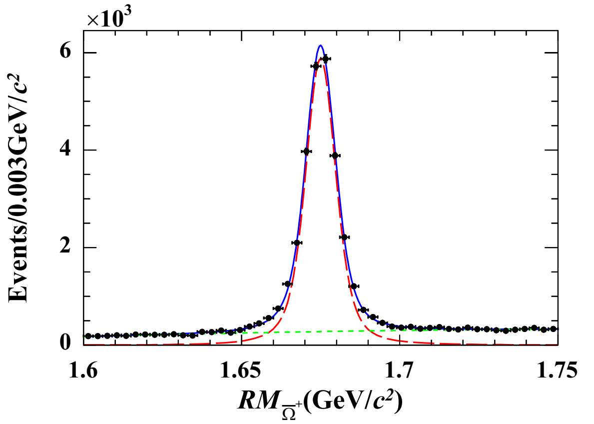

FIG. 1. Fit to the $RM_{\bar{\Omega}^+}$ distribution. The dots with error bars are data, the blue solid line is the total fit, and the green short-dashed and magenta long-dashed lines represent the fitted background and signal shapes, respectively.

Events in the $\bar{\Omega}^+$ sideband region, defined as $M_{\bar{\Lambda}K^+} \in [1.648, 1.656] \cup [1.688, 1.696]$ GeV$/c^2$, are used to study the potential peaking backgrounds in data. No peaking background is found. To determine the ST yields, an unbinned maximum-likelihood fit is performed to the recoil-mass spectrum against the reconstructed $\bar{\Omega}^+$ ($RM_{\bar{\Omega}^+}$), as shown in Fig. 1. In the fit, the signal shape is described by the MC simulated shape convolved with a Gaussian function with free parameters, where the Gaussian function is used to compensate for the difference in mass resolution between data and MC simulation. The background shape is described by a second-order Chebyshev polynomial. The signal region of $RM_{\bar{\Omega}^+}$ is defined as $[1.652, 1.695]$ GeV$/c^2$, and the number of ST $\bar{\Omega}^+$ baryons is 25819 ± 188, with a corresponding efficiency of 23.55%, as listed in Table I.

The $\pi^-(\pi^0)$ candidates from the decay $\Omega^- \to \Xi^0\pi^-(\Xi^-\pi^0)$ are reconstructed in the recoil side of the $\bar{\Omega}^+$. The tracks that satisfy $|\cos\theta| < 0.93$ and $\mathcal{L}(\pi) > \mathcal{L}(K)$ are regarded as pion candidates. The photons used to reconstruct the π^0 candidates are detected in the EMC. Each photon is required to have an EMC energy deposit of more than 25 MeV in the barrel region ($|\cos\theta| < 0.80$) or more than 50 MeV in the end-cap region ($0.86 < |\cos\theta| < 0.92$). To suppress electronic noise and showers unrelated to the event, the difference between the EMC time and the event start time is required to be within (0, 700) ns. Furthermore, to reject showers that originate from charged tracks, the angle between the shower and its

TABLE I. The ST yields (N_{ST}), ST efficiency (ϵ_{ST}), DT yields (N_{DT}), DT efficiency (ϵ_{DT}) and the absolute BFs of the three dominant Ω^- decays, $\Omega^- \to \Xi^0\pi^-$, $\Omega^- \to \Xi^-\pi^0$, and $\Omega^- \to \Lambda K^-(\bar{\Omega}^+ \to \bar{\Lambda}K^+)$. Here the uncertainties are statistical only.

Decay mode	N_{ST}	ϵ_{ST} (%)	N_{DT}	ϵ_{DT} (%)	BF (%)
$\Omega^- \to \Xi^0\pi^-$	25819 ± 188	23.55	5411 ± 95	19.72	25.03 ± 0.44
$\Omega^- \to \Xi^-\pi^0$			794 ± 49	8.59	8.43 ± 0.52
$\Omega^- \to \Lambda K^-$	12111 ± 127	22.78	4877 ± 72	13.64	67.25 ± 0.99
$\bar{\Omega}^+ \to \bar{\Lambda}K^+$	13705 ± 139	24.31	5427 ± 78	14.75	65.26 ± 0.94

closest charged track must be greater than 10°. The photons are combined into pairs and at least one photon is required to come from the barrel region. The photon pairs with invariant mass within the range $[0.115, 0.150]$ GeV$/c^2$ are denoted as π^0 candidates. A kinematic fit [32] constraining the $\gamma\gamma$ invariant mass to the known π^0 mass [13] is performed, and the resulting χ^2 must be less than 200. If there is more than one $\pi^-(\pi^0)$ candidate, the one with the highest energy is kept for further analysis.

For the measurement of $\mathcal{B}_{\Omega^-\to\Xi^-\pi^0}$, it is necessary to veto the background from the decays $\Omega^- \to \Lambda K^-$ and $\Omega^- \to \Xi^0\pi^-$, which also have π^0s in the signal side. To veto the background from $\Omega^- \to \Xi^0\pi^-$, if the highest momentum track on the signal side carries the opposite charge to the tagged $\bar{\Omega}^+$, it is assigned as a pion and the recoil mass against the $\bar{\Omega}^+\pi^-$ system, $RM_{\bar{\Omega}^+\pi^-}$, is calculated. We require $RM_{\bar{\Omega}^+\pi^-} > 1.38$ GeV$/c^2$ to exclude events from $\Omega^- \to \Xi^0\pi^-$, where there would be a peak around the known Ξ^0 mass in the $RM_{\bar{\Omega}^+\pi^-}$ spectrum. For the background from $\Omega^- \to \Lambda K^-$, if there are K^- tracks on the signal side, the K^- with the highest $\mathcal{L}(K)$ is used to calculate the recoil mass against the $\bar{\Omega}^+K^-$ system, $RM_{\bar{\Omega}^+K^-}$, and $RM_{\bar{\Omega}^+K^-} > 1.2$ GeV$/c^2$ is required to veto this background.

Potential peaking backgrounds in the measurements of $\mathcal{B}_{\Omega^-\to\Xi^0\pi^-}$ and $\mathcal{B}_{\Omega^-\to\Xi^-\pi^0}$ are investigated by analyzing the inclusive MC sample and the events in the $M_{\bar{\Lambda}K^+}$ or $RM_{\bar{\Omega}^+}$ sideband regions from data. The $RM_{\bar{\Omega}^+}$ sideband region is defined as $RM_{\bar{\Omega}^+} \in [1.608, 1.630] \cup [1.718, 1.739]$ GeV$/c^2$. The number of peaking background events is estimated to be 46 ± 20 for the $\Omega^- \to \Xi^0\pi^-$ mode, while there is no peaking background for the $\Omega^- \to \Xi^-\pi^0$ mode.

For the signal events of the DT sample, the recoil-mass spectrum against the $\bar{\Omega}^+\pi^-(\bar{\Omega}^+\pi^0)$ system, $RM_{\bar{\Omega}^+\pi^-}(RM_{\bar{\Omega}^+\pi^0})$, peaks around the $\Xi^0(\Xi^-)$ mass. An unbinned maximum-likelihood fit is performed on $RM_{\bar{\Omega}^+\pi^-}(RM_{\bar{\Omega}^+\pi^0})$ to determine the DT yields, as shown in Fig. 2. In the fit, the signal shape is described by the MC simulated shape convolved with a Gaussian function. To obtain the MC simulated shape of $RM_{\bar{\Omega}^+\pi^0}$, a truth matching method is used, where the opening angle between the reconstructed and MC-truth momentum directions of π^0 is required to be less than 10° and the energy difference between them is required to be less than 0.1 GeV. The background shape is described by a second-order Chebyshev polynomial. After subtracting the number of peaking background events, the number of DT events of the $\bar{\Omega}^+\pi^-(\bar{\Omega}^+\pi^0)$ sample is determined to be $5411 \pm 95(794 \pm 49)$, as listed in Table I. The polar angle and energy distributions of π^0 in data from $\Omega^- \to \Xi^-\pi^0$ are well described by the PHSP model. The polar angle distribution of π^- from $\Omega^- \to \Xi^0\pi^-$ is also consistent between data and MC simulation, while the transverse momentum distributions of π^- (p_{T,π^-}) is not. To obtain a more accurate DT efficiency in the measurement of $\mathcal{B}_{\Omega^-\to\Xi^0\pi^-}$, the events of the signal MC sample are weighted according to the p_{T,π^-} distribution in data. The weight factors are the ratios $n^i_{\mathrm{data}}/n^i_{\mathrm{MC}}$ which are obtained in different p_{T,π^-} bins, where n^i_{data} and n^i_{MC} are the numbers of DT $\bar{\Omega}^+\pi^-$ candidates in the i-th p_{T,π^-} bin from data and MC samples, respectively. The resultant DT efficiencies are 19.72% and 8.59% for $\bar{\Omega}^+\pi^-$ and $\bar{\Omega}^+\pi^0$, respectively, as listed in Table I.

The absolute BFs of $\Omega^- \to \Xi^0\pi^-$ and $\Omega^- \to \Xi^-\pi^0$ are determined to be $\mathcal{B}_{\Omega^-\to\Xi^0\pi^-} = (25.03 \pm 0.44)\%$ and $\mathcal{B}_{\Omega^-\to\Xi^-\pi^0} = (8.43 \pm 0.52)\%$, respectively, as listed in Table I. Here, the uncertainties are statistical only.

For the $\Omega^- \to \Lambda K^-$ channel, the BFs ($\mathcal{B}_{\Omega^-\to\Lambda K^-}$) of the charge conjugate modes $\Omega^- \to \Lambda K^-$ and $\bar{\Omega}^+ \to \bar{\Lambda}K^+$ are determined separately, since we observe the same decay mode of $\Omega \to \Lambda K$ on both the tag and signal sides. In this channel, the selection criteria of the ST events are the same as those in the $\Omega^- \to \Xi^0\pi^-(\Xi^-\pi^0)$ BF measurement. The ST yield is determined to be $12111 \pm 127(13705 \pm 139)$,

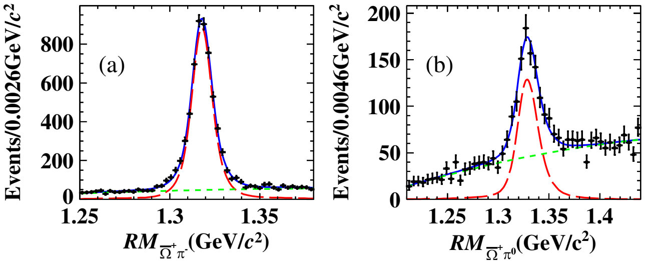

FIG. 2. Fits to the distributions of (a) $RM_{\bar{\Omega}^+\pi^-}$ and (b) $RM_{\bar{\Omega}^+\pi^0}$. The dots with error bars are data, the blue solid line is the total fit, and the green short-dashed and magenta long-dashed lines represent the fitted background and signal shapes, respectively.

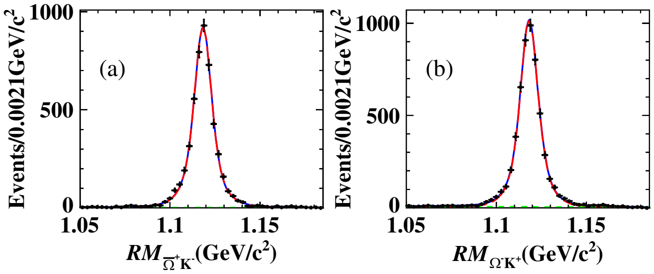

FIG. 3. Fits to the distributions of (a) $RM_{\bar{\Omega}^+K^-}$ and (b) $RM_{\Omega^-K^+}$. The dots with error bars are data, the blue solid line is the total fit, and the green short-dashed and magenta long-dashed lines represent the fitted background and signal shapes, respectively.

and the ST efficiency is 22.78% (24.31%) for the tagged $\bar{\Omega}^+(\Omega^-)$, as listed in Table I.

For the signal side, at least one good charged $K^-(K^+)$ track is required. If there is more than one $K^-(K^+)$, the one with the highest $\mathcal{L}(K)$ is kept for further study. Potential peaking backgrounds for the DT events in the measurement of $\mathcal{B}_{\Omega^-\to\Lambda K^-}$ are investigated by analyzing the inclusive MC sample and the events in the $M_{\bar{\Lambda}K^+}(M_{\Lambda K^-})$ or $RM_{\bar{\Omega}^+}(RM_{\Omega^-})$ sideband regions from data. We find $22\pm7(24\pm9)$ peaking background events for the DT $\bar{\Omega}^+K^-(\Omega^-K^+)$ sample.

For the signal events of the DT sample, the recoil-mass spectrum against the $\bar{\Omega}^+K^-(\Omega^-K^+)$ system, $RM_{\bar{\Omega}^+K^-}(RM_{\Omega^-K^+})$, should peak around the $\Lambda(\bar{\Lambda})$ mass. Therefore, an unbinned maximum-likelihood fit is performed on $RM_{\bar{\Omega}^+K^-}(RM_{\Omega^-K^+})$ to determine the DT yield, as shown in Fig. 3. In the fit, the signal shape is described by the MC simulated shape convolved with a Gaussian function. The background shape is described by a first-order Chebyshev polynomial. After subtracting the number of peaking background events, the number of DT events of $\Omega^-\to\Lambda K^-(\bar{\Omega}^+\to\bar{\Lambda}K^+)$ is determined to be 4877 ± 72 (5427 ± 78), as listed in Table I. Similar to the pion case, the PHSP model also cannot correctly simulate the $K^-(K^+)$ transverse momentum distribution. To obtain a more accurate DT efficiency, the events of the PHSP MC sample are weighted according to the observed distribution of $K^-(K^+)$ transverse momentum. The resulting DT efficiency is determined to be 13.64% (14.75%), as listed in Table I.

The absolute BFs of the charge separated decays $\Omega^-\to\Lambda K^-$ and $\bar{\Omega}^+\to\bar{\Lambda}K^+$ are determined to be $\mathcal{B}^{\Omega^-}_{\Lambda K^-}=(67.25\pm0.99)\%$ and $\mathcal{B}^{\bar{\Omega}^+}_{\bar{\Lambda}K^+}=(65.26\pm0.94)\%$, respectively, as listed in Table I. Weighting these two BFs and considering the correlation of the 1292 overlap events between the $\bar{\Omega}^+K^-$ and Ω^-K^+ samples [33], we obtain the average BF of $\mathcal{B}_{\Omega^-\to\Lambda K^-}=(66.3\pm0.8)\%$, where the uncertainty is statistical only.

With the DT method, most uncertainties related to the ST selection cancel. The sources of the systematic uncertainties are summarized in Table II. Each of them is described in the following paragraphs.

TABLE II. BF Relative systematic uncertainties in %.

Source	$\mathcal{B}_{\Omega^-\to\Xi^0\pi^-}$	$\mathcal{B}_{\Omega^-\to\Xi^-\pi^0}$	$\mathcal{B}_{\Omega^-\to\Lambda K^-}$
Photon detection	⋯	2.0	⋯
π^0 reconstruction	⋯	1.0	⋯
Pion/kaon tracking	0.3	⋯	1.0
Pion/kaon PID	0.2	⋯	1.0
ST signal shape	0.9	0.9	0.9
DT signal shape	0.0	1.4	0.2
ST background shape	0.7	0.7	0.7
DT background shape	0.2	0.9	0.8
ST background fluctuation	0.4	0.4	0.4
Weighting procedure	1.7	⋯	2.2
$\Xi^0\pi^-$ veto	⋯	1.3	⋯
Truth match	⋯	0.5	⋯
MC statistics	0.1	0.2	0.1
Total	2.1	3.3	3.0

The systematic uncertainty associated with the photon reconstruction efficiency is estimated to be 1.0% per photon [34], while that due to the π^0 reconstruction is also 1.0% [35]. The uncertainties arising from the tracking and PID efficiencies are both 1.0% per kaon track [36]. A control sample $J/\psi\to p\bar{p}\pi^+\pi^-$ is used to estimate the uncertainties of the pion tracking and PID efficiencies. The efficiency differences between data and MC simulation for the control sample are used to reweight the signal MC sample of $\Omega^-\to\Xi^0\pi^-$. The differences between the nominal and re-weighted detection efficiencies are taken as the systematic uncertainties, which are 0.3% and 0.2% for pion tracking and PID efficiencies, respectively.

The uncertainties associated with the ST and DT signal shapes are estimated by replacing the Gaussian resolution function with a double-Gaussian function. The differences in the signal yields are taken as the systematic uncertainties, which are 0.9% for the ST yield, and 0.0%, 1.4%, and 0.2% for the DT yields of $\Omega^-\to\Xi^0\pi^-$, $\Omega^-\to\Xi^-\pi^0$, and $\Omega^-\to\Lambda K^-$, respectively. The uncertainty due to the ST background shape is studied by changing the second-order Chebyshev polynomial to a first-order or third-order Chebyshev polynomial, and the largest difference on the ST yield, 0.7%, is taken as the uncertainty. The uncertainties caused by the DT background shapes are investigated by increasing the order of the nominal Chebyshev polynomial by one, and the changes of the DT yields are taken as the systematic uncertainties, which are 0.2%, 0.9%, and 0.8% for $\Omega^-\to\Xi^0\pi^-$, $\Omega^-\to\Xi^-\pi^0$, and $\Omega^-\to\Lambda K^-$, respectively. In addition, the uncertainty due to the background fluctuation of the ST yield, 0.4%, is also considered as a systematic uncertainty.

To obtain reliable signal efficiencies, the signal MC samples of $\Omega^-\to\Xi^0\pi^-$ and $\Omega^-\to\Lambda K^-$ are weighted to match the data. To estimate the associated systematic uncertainty, the weight factors are randomly changed within one standard deviation in each bin one thousand

TABLE III. The obtained BFs (in %) and comparison with the PDG values. The first and second uncertainties presented in this work are statistical and systematic, respectively.

BFs	$\mathcal{B}_{\Omega^-\to\Xi^0\pi^-}$	$\mathcal{B}_{\Omega^-\to\Xi^-\pi^0}$	$\mathcal{B}_{\Omega^-\to\Lambda K^-}$
This work	$25.03 \pm 0.44 \pm 0.53$	$8.43 \pm 0.52 \pm 0.28$	$66.3 \pm 0.8 \pm 2.0$
PDG	23.6 ± 0.7	8.6 ± 0.4	67.8 ± 0.7

times to reobtain the DT efficiencies. The distributions of the resulting DT efficiencies are fit with Gaussian functions, and their standard deviations are taken as the systematic uncertainties, which are 1.7% and 2.2% for $\Omega^- \to \Xi^0\pi^-$ and $\Omega^- \to \Lambda K^-$, respectively.

The systematic uncertainty of vetoing the background of $\Omega^- \to \Xi^0\pi^-$ in the measurement of $\mathcal{B}_{\Omega^-\to\Xi^-\pi^0}$ is studied by varying this requirement from $RM_{\bar{\Omega}^+\pi^-} > 1.38\ \mathrm{GeV}/c^2$ to $RM_{\bar{\Omega}^+\pi^-} > 1.36\ \mathrm{GeV}/c^2$ or $RM_{\bar{\Omega}^+\pi^-} > 1.40\ \mathrm{GeV}/c^2$. The resulting largest difference to the original BF, 1.3%, is taken as the systematic uncertainty. Since there is no signal efficiency loss of vetoing the background of $\Omega^- \to \Lambda K^-$, the systematic uncertainty due to this requirement is negligible.

The systematic uncertainty of the truth matching method in the $\Omega^- \to \Xi^-\pi^0$ mode originates from the requirements on the opening angle between the reconstructed and MC-truth momentum directions of the π^0, and the energy difference between the reconstructed and MC-truth π^0s. The relevant uncertainties are estimated by varying the opening angle value to be 5° or 15°, and the energy difference to be 0.05 GeV or 0.15 GeV. The resulting largest difference to the original BF is assigned as the uncertainty, which is 0.5%.

The uncertainties due to the MC statistics are estimated to be 0.1%, 0.2%, and 0.1% for $\Omega^- \to \Xi^0\pi^-$, $\Omega^- \to \Xi^-\pi^0$, and $\Omega^- \to \Lambda K^-$, respectively.

Adding these systematic uncertainties in quadrature, we obtain the total systematic uncertainties for the measurements of $\mathcal{B}_{\Omega^-\to\Xi^0\pi^-}$, $\mathcal{B}_{\Omega^-\to\Xi^-\pi^0}$, and $\mathcal{B}_{\Omega^-\to\Lambda K^-}$ to be 2.1%, 3.3%, and 3.0%, respectively.

In summary, utilizing $(27.12 \pm 0.10) \times 10^8$ $\psi(3686)$ events collected with the BESIII detector, the absolute BFs of $\Omega^- \to \Xi^0\pi^-$, $\Omega^- \to \Xi^-\pi^0$, and $\Omega^- \to \Lambda K^-$ have been measured. The results are shown in Table III. The ratio between $\mathcal{B}_{\Omega^-\to\Xi^0\pi^-}$ and $\mathcal{B}_{\Omega^-\to\Xi^-\pi^0}$ is determined to be $2.97 \pm 0.19 \pm 0.11$, where the systematic uncertainties associated with the ST yields cancel in the calculation. Our result is consistent with the PDG value 2.74 ± 0.15 (combining statistical and systematic uncertainties in quadrature), but differs from the expectation (equal to 2) based on the $\Delta I = 1/2$ rule by more than four standard deviations. Our measurement and the PDG value both suggest a surprisingly strong admixture of a $\Delta I = 3/2$ amplitude, which is very different from the behavior observed in other measured weak decays, especially the decays of the octet baryons [6]. To understand this phenomenon, the current effective-field-theory picture about the interplay of the strong and weak interactions needs to be improved [16].

The BESIII Collaboration thanks the staff of BEPCII and the IHEP computing center for their strong support. This work is supported in part by National Key R&D Program of China under Contracts No. 2020YFA0406300, No. 2020YFA0406400; National Natural Science Foundation of China (NSFC) under Contracts No. 11635010, No. 11735014, No. 11835012, No. 11935015, No. 11935016, No. 11935018, No. 11961141012, No. 12022510, No. 12025502, No. 12035009, No. 12035013, No. 12061131003, No. 12192260, No. 12192261, No. 12192262, No. 12192263, No. 12192264, No. 12192265, No. 12221005, No. 12225509, No. 12235017; the Chinese Academy of Sciences (CAS) Large-Scale Scientific Facility Program; the CAS Center for Excellence in Particle Physics (CCEPP); Joint Large-Scale Scientific Facility Funds of the NSFC and CAS under Contract No. U1832207; CAS Key Research Program of Frontier Sciences under Contracts No. QYZDJ-SSW-SLH003, No. QYZDJ-SSW-SLH040; 100 Talents Program of CAS; The Institute of Nuclear and Particle Physics (INPAC) and Shanghai Key Laboratory for Particle Physics and Cosmology; ERC under Contract No. 758462; European Union's Horizon 2020 research and innovation programme under Marie Sklodowska-Curie grant agreement under Contract No. 894790; German Research Foundation DFG under Contracts Nos. 455635585, Collaborative Research Center CRC 1044, FOR5327, GRK 2149; Istituto Nazionale di Fisica Nucleare, Italy; Ministry of Development of Turkey under Contract No. DPT2006K-120470; National Research Foundation of Korea under Contract No. NRF-2022R1A2C1092335; National Science and Technology fund of Mongolia; National Science Research and Innovation Fund (NSRF) via the Program Management Unit for Human Resources & Institutional Development, Research and Innovation of Thailand under Contract No. B16F640076; Polish National Science Centre under Contract No. 2019/35/O/ST2/02907; The Swedish Research Council; U.S. Department of Energy under Contract No. DE-FG02-05ER41374.

[1] V. E. Barnes *et al.*, Phys. Rev. Lett. **12**, 204 (1964).

[2] B. Aubert *et al.* (*BABAR* Collaboration), Phys. Rev. Lett. **97**, 112001 (2006).

[3] M. Ablikim *et al.* (BESIII Collaboration), Phys. Rev. Lett. **126**, 092002 (2021).

[4] D. N. Goswami and J. Schechter, Phys. Rev. D **1**, 290 (1970); **4**, 3526(E) (1971).

[5] C. Carone and H. Georgi, Nucl. Phys. **B375**, 243 (1992).

[6] J. Tandean and G. Valencia, Phys. Lett. B **452**, 395 (1999).

[7] D. A. Egolf, I. V. Melnikov, and R. P. Springer, Phys. Lett. B **451**, 267 (1999).

[8] O. Antipin, J. Tandean, and G. Valencia, Phys. Rev. D **76**, 094024 (2007).

[9] H. Georgi, *Weak Interactions and Modern Particle Theory* (Dover Publications, New York, 1984), ISBN-10 0486469042.

[10] E. E. Jenkins, Nucl. Phys. **B375**, 561 (1992).

[11] V. Cirigliano, G. Ecker, H. Neufeld, A. Pich, and J. Portoles, Rev. Mod. Phys. **84**, 399 (2012).

[12] N. Salone, P. Adlarson, V. Batozskaya, A. Kupsc, S. Leupold, and J. Tandean, Phys. Rev. D **105**, 116022 (2022).

[13] R. L. Workman *et al.* (Particle Data Group), Prog. Theor. Exp. Phys. **2022**, 083C01 (2022).

[14] O. E. Overseth and S. Pakvasa, Phys. Rev. **184**, 1663 (1969).

[15] M. Bourquin *et al.* (Bristol-Geneva-Heidelberg-Orsay-Rutherford-Strasbourg Collaboration), Nucl. Phys. **B241**, 1 (1984).

[16] C. J. G. Mommers and S. Leupold, Phys. Rev. D **106**, 093001 (2022).

[17] H. B. Li, Front. Phys. (Beijing) **12**, 121301 (2017); **14**, 64001(E) (2019).

[18] M. Ablikim *et al.* (BESIII Collaboration), Chin. Phys. C **42**, 023001 (2018), the total number of $\psi(3686)$ events collected in 2009, 2012 and 2021 is determined to be 27.12×10^8 with an uncertainty of 0.4% as a preliminary result.

[19] M. Ablikim *et al.*, Nucl. Instrum. Methods Phys. Res., Sect. A **614**, 345 (2010).

[20] C. H. Yu *et al.*, in *Proceedings of IPAC2016, Busan, Korea* (2016), 10.18429/JACoW-IPAC2016-TUYA01.

[21] M. Ablikim *et al.* (BESIII Collaboration), Chin. Phys. C **44**, 040001 (2020).

[22] K. X. Huang, Z. J. Li, Z. Qian, J. Zhu, H. Y. Li, Y. M. Zhang, S. S. Sun, and Z. Y. You, Nucl. Sci. Tech. **33**, 142 (2022).

[23] X. Li *et al.*, Nucl. Sci. Tech. **1**, 13 (2017).

[24] Y. X. Guo *et al.*, Nucl. Sci. Tech. **1**, 15 (2017).

[25] P. Cao *et al.*, Nucl. Instrum. Methods Phys. Res., Sect. A **953**, 163053 (2020).

[26] S. Agostinelli *et al.*, Nucl. Instrum. Methods Phys. Res., Sect. A **506**, 250 (2003).

[27] Z. Y. Deng *et al.*, Chin. Phys. C **30**, 371 (2006), http://cpc.ihep.ac.cn/article/id/283d17c0-e8fa-4ad7-bfe3-92095466def1.

[28] S. Jadach, B. F. L. Ward, and Z. Was, Phys. Rev. D **63**, 113009 (2001).

[29] D. J. Lange, Nucl. Instrum. Methods Phys. Res., Sect. A **462**, 152 (2001); R. G. Ping, Chin. Phys. C **32**, 599 (2008).

[30] J. C. Chen, G. S. Huang, X. R. Qi, D. H. Zhang, and Y. S. Zhu, Phys. Rev. D **62**, 034003 (2000); R. L. Yang, R. G. Ping, and H. Chen, Chin. Phys. Lett. **31**, 061301 (2014).

[31] E. Richter Was, Phys. Lett. B **303**, 163 (1993).

[32] L. Yan *et al.*, Chin. Phys. C **34**, 204 (2010).

[33] F. James, *Statistical Methods in Experimental Physics* (World Scientific, Singapore, 2006), ISBN 9789812567956, 9789812705273.

[34] M. Ablikim *et al.* (BESIII Collaboration), Phys. Rev. D **83**, 012006 (2011).

[35] M. Ablikim *et al.* (BESIII Collaboration), Phys. Rev. D **81**, 052005 (2010).

[36] M. Ablikim *et al.* (BESIII Collaboration), Phys. Rev. D **99**, 032001 (2019).

M. Ablikim,[1] M. N. Achasov,[5,b] P. Adlarson,[74] X. C. Ai,[80] R. Aliberti,[35] A. Amoroso,[73a,73c] M. R. An,[39] Q. An,[70,57] Y. Bai,[56] O. Bakina,[36] I. Balossino,[29a] Y. Ban,[46,g] V. Batozskaya,[1,44] K. Begzsuren,[32] N. Berger,[35] M. Berlowski,[44] M. Bertani,[28a] D. Bettoni,[29a] F. Bianchi,[73a,73c] E. Bianco,[73a,73c] A. Bortone,[73a,73c] I. Boyko,[36] R. A. Briere,[6] A. Brueggemann,[67] H. Cai,[75] X. Cai,[1,57] A. Calcaterra,[28a] G. F. Cao,[1,62] N. Cao,[1,62] S. A. Cetin,[61a] J. F. Chang,[1,57] T. T. Chang,[76] W. L. Chang,[1,62] G. R. Che,[43] G. Chelkov,[36,a] C. Chen,[43] Chao Chen,[54] G. Chen,[1] H. S. Chen,[1,62] M. L. Chen,[1,57,62] S. J. Chen,[42] S. M. Chen,[60] T. Chen,[1,62] X. R. Chen,[31,62] X. T. Chen,[1,62] Y. B. Chen,[1,57] Y. Q. Chen,[34] Z. J. Chen,[25,h] W. S. Cheng,[73c] S. K. Choi,[11] X. Chu,[43] G. Cibinetto,[29a] S. C. Coen,[4] F. Cossio,[73c] J. J. Cui,[49] H. L. Dai,[1,57] J. P. Dai,[78] A. Dbeyssi,[18] R. E. de Boer,[4] D. Dedovich,[36] Z. Y. Deng,[1] A. Denig,[35] I. Denysenko,[36] M. Destefanis,[73a,73c] F. De Mori,[73a,73c] B. Ding,[65,1] X. X. Ding,[46,g] Y. Ding,[40] Y. Ding,[34] J. Dong,[1,57] L. Y. Dong,[1,62] M. Y. Dong,[1,57,62] X. Dong,[75] M. C. Du,[1] S. X. Du,[80] Z. H. Duan,[42] P. Egorov,[36,a] Y. H. Y. Fan,[45] Y. L. Fan,[75] J. Fang,[1,57] S. S. Fang,[1,62] W. X. Fang,[1] Y. Fang,[1] R. Farinelli,[29a] L. Fava,[73b,73c] F. Feldbauer,[4] G. Felici,[28a] C. Q. Feng,[70,57] J. H. Feng,[58] K Fischer,[68] M. Fritsch,[4] C. Fritzsch,[67] C. D. Fu,[1] J. L. Fu,[62] Y. W. Fu,[1] H. Gao,[62] Y. N. Gao,[46,g] Yang Gao,[70,57] S. Garbolino,[73c] I. Garzia,[29a,29b] P. T. Ge,[75] Z. W. Ge,[42] C. Geng,[58] E. M. Gersabeck,[66] A Gilman,[68] K. Goetzen,[14] L. Gong,[40] W. X. Gong,[1,57] W. Gradl,[35] S. Gramigna,[29a,29b] M. Greco,[73a,73c] M. H. Gu,[1,57] C. Y Guan,[1,62] Z. L. Guan,[22] A. Q. Guo,[31,62] L. B. Guo,[41] M. J. Guo,[49] R. P. Guo,[48] Y. P. Guo,[13,f] A. Guskov,[36,a] T. T. Han,[49] W. Y. Han,[39] X. Q. Hao,[19] F. A. Harris,[64] K. K. He,[54] K. L. He,[1,62] F. H. H. Heinsius,[4] C. H. Heinz,[35] Y. K. Heng,[1,57,62] C. Herold,[59] T. Holtmann,[4] P. C. Hong,[13,f] G. Y. Hou,[1,62] X. T. Hou,[1,62] Y. R. Hou,[62] Z. L. Hou,[1] H. M. Hu,[1,62] J. F. Hu,[55,i] T. Hu,[1,57,62] Y. Hu,[1] G. S. Huang,[70,57] K. X. Huang,[58] L. Q. Huang,[31,62] X. T. Huang,[49]

Y. P. Huang,[1] T. Hussain,[72] N Hüsken,[27,35] W. Imoehl,[27] J. Jackson,[27] S. Jaeger,[4] S. Janchiv,[32] J. H. Jeong,[11] Q. Ji,[1] Q. P. Ji,[19] X. B. Ji,[1,62] X. L. Ji,[1,57] Y. Y. Ji,[49] X. Q. Jia,[49] Z. K. Jia,[70,57] H. J. Jiang,[75] P. C. Jiang,[46,g] S. S. Jiang,[39] T. J. Jiang,[16] X. S. Jiang,[1,57,62] Y. Jiang,[62] J. B. Jiao,[49] Z. Jiao,[23] S. Jin,[42] Y. Jin,[65] M. Q. Jing,[1,62] T. Johansson,[74] X. K.,[1] S. Kabana,[33] N. Kalantar-Nayestanaki,[63] X. L. Kang,[10] X. S. Kang,[40] M. Kavatsyuk,[63] B. C. Ke,[80] A. Khoukaz,[67] R. Kiuchi,[1] R. Kliemt,[14] O. B. Kolcu,[61a] B. Kopf,[4] M. Kuessner,[4] A. Kupsc,[44,74] W. Kühn,[37] J. J. Lane,[66] P. Larin,[18] A. Lavania,[26] L. Lavezzi,[73a,73c] T. T. Lei,[70,57] Z. H. Lei,[70,57] H. Leithoff,[35] M. Lellmann,[35] T. Lenz,[35] C. Li,[43] C. Li,[47] C. H. Li,[39] Cheng Li,[70,57] D. M. Li,[80] F. Li,[1,57] G. Li,[1] H. Li,[70,57] H. B. Li,[1,62] H. J. Li,[19] H. N. Li,[55,i] Hui Li,[43] J. R. Li,[60] J. S. Li,[58] J. W. Li,[49] K. L. Li,[19] Ke Li,[1] L. J Li,[1,62] L. K. Li,[1] Lei Li,[3] M. H. Li,[43] P. R. Li,[38,j,k] Q. X. Li,[49] S. X. Li,[13] T. Li,[49] W. D. Li,[1,62] W. G. Li,[1] X. H. Li,[70,57] X. L. Li,[49] Xiaoyu Li,[1,62] Y. G. Li,[46,g] Z. J. Li,[58] C. Liang,[42] H. Liang,[70,57] H. Liang,[34] H. Liang,[1,62] Y. F. Liang,[53] Y. T. Liang,[31,62] G. R. Liao,[15] L. Z. Liao,[49] Y. P. Liao,[1,62] J. Libby,[26] A. Limphirat,[59] D. X. Lin,[31,62] T. Lin,[1] B. J. Liu,[1] B. X. Liu,[75] C. Liu,[34] C. X. Liu,[1] F. H. Liu,[52] Fang Liu,[1] Feng Liu,[7] G. M. Liu,[55,i] H. Liu,[38,j,k] H. M. Liu,[1,62] Huanhuan Liu,[1] Huihui Liu,[21] J. B. Liu,[70,57] J. L. Liu,[71] J. Y. Liu,[1,62] K. Liu,[1] K. Y. Liu,[40] Ke Liu,[22] L. Liu,[70,57] L. C. Liu,[43] Lu Liu,[43] M. H. Liu,[13,f] P. L. Liu,[1] Q. Liu,[62] S. B. Liu,[70,57] T. Liu,[13,f] W. K. Liu,[43] W. M. Liu,[70,57] X. Liu,[38,j,k] Y. Liu,[38,j,k] Y. Liu,[80] Y. B. Liu,[43] Z. A. Liu,[1,57,62] Z. Q. Liu,[49] X. C. Lou,[1,57,62] F. X. Lu,[58] H. J. Lu,[23] J. G. Lu,[1,57] X. L. Lu,[1] Y. Lu,[8] Y. P. Lu,[1,57] Z. H. Lu,[1,62] C. L. Luo,[41] M. X. Luo,[79] T. Luo,[13,f] X. L. Luo,[1,57] X. R. Lyu,[62] Y. F. Lyu,[43] F. C. Ma,[40] H. L. Ma,[1] J. L. Ma,[1,62] L. L. Ma,[49] M. M. Ma,[1,62] Q. M. Ma,[1] R. Q. Ma,[1,62] R. T. Ma,[62] X. Y. Ma,[1,57] Y. Ma,[46,g] Y. M. Ma,[31] F. E. Maas,[18] M. Maggiora,[73a,73c] S. Malde,[68] Q. A. Malik,[72] A. Mangoni,[28b] Y. J. Mao,[46,g] Z. P. Mao,[1] S. Marcello,[73a,73c] Z. X. Meng,[65] J. G. Messchendorp,[14,63] G. Mezzadri,[29a] H. Miao,[1,62] T. J. Min,[42] R. E. Mitchell,[27] X. H. Mo,[1,57,62] N. Yu. Muchnoi,[5,b] J. Muskalla,[35] Y. Nefedov,[36] F. Nerling,[18,d] I. B. Nikolaev,[5,b] Z. Ning,[1,57] S. Nisar,[12,l] W. D. Niu,[54] Y. Niu,[49] S. L. Olsen,[62] Q. Ouyang,[1,57,62] S. Pacetti,[28b,28c] X. Pan,[54] Y. Pan,[56] A. Pathak,[34] P. Patteri,[28a] Y. P. Pei,[70,57] M. Pelizaeus,[4] H. P. Peng,[70,57] K. Peters,[14,d] J. L. Ping,[41] R. G. Ping,[1,62] S. Plura,[35] S. Pogodin,[36] V. Prasad,[33] F. Z. Qi,[1] H. Qi,[70,57] H. R. Qi,[60] M. Qi,[42] T. Y. Qi,[13,f] S. Qian,[1,57] W. B. Qian,[62] C. F. Qiao,[62] J. J. Qin,[71] L. Q. Qin,[15] X. P. Qin,[13,f] X. S. Qin,[49] Z. H. Qin,[1,57] J. F. Qiu,[1] S. Q. Qu,[60] C. F. Redmer,[35] K. J. Ren,[39] A. Rivetti,[73c] M. Rolo,[73c] G. Rong,[1,62] Ch. Rosner,[18] S. N. Ruan,[43] N. Salone,[44] A. Sarantsev,[36,c] Y. Schelhaas,[35] K. Schoenning,[74] M. Scodeggio,[29a,29b] K. Y. Shan,[13,f] W. Shan,[24] X. Y. Shan,[70,57] J. F. Shangguan,[54] L. G. Shao,[1,62] M. Shao,[70,57] C. P. Shen,[13,f] H. F. Shen,[1,62] W. H. Shen,[62] X. Y. Shen,[1,62] B. A. Shi,[62] H. C. Shi,[70,57] J. L. Shi,[13] J. Y. Shi,[1] Q. Q. Shi,[54] R. S. Shi,[1,62] X. Shi,[1,57] J. J. Song,[19] T. Z. Song,[58] W. M. Song,[34,1] Y. J. Song,[13] Y. X. Song,[46,g] S. Sosio,[73a,73c] S. Spataro,[73a,73c] F. Stieler,[35] Y. J. Su,[62] G. B. Sun,[75] G. X. Sun,[1] H. Sun,[62] H. K. Sun,[1] J. F. Sun,[19] K. Sun,[60] L. Sun,[75] S. S. Sun,[1,62] T. Sun,[1,62] W. Y. Sun,[34] Y. Sun,[10] Y. J. Sun,[70,57] Y. Z. Sun,[1] Z. T. Sun,[49] Y. X. Tan,[70,57] C. J. Tang,[53] G. Y. Tang,[1] J. Tang,[58] Y. A. Tang,[75] L. Y Tao,[71] Q. T. Tao,[25,h] M. Tat,[68] J. X. Teng,[70,57] V. Thoren,[74] W. H. Tian,[51] W. H. Tian,[58] Y. Tian,[31,62] Z. F. Tian,[75] I. Uman,[61b] S. J. Wang,[49] B. Wang,[1] B. L. Wang,[62] Bo Wang,[70,57] C. W. Wang,[42] D. Y. Wang,[46,g] F. Wang,[71] H. J. Wang,[38,j,k] H. P. Wang,[1,62] J. P. Wang,[49] K. Wang,[1,57] L. L. Wang,[1] M. Wang,[49] Meng Wang,[1,62] S. Wang,[13,f] S. Wang,[38,j,k] T. Wang,[13,f] T. J. Wang,[43] W. Wang,[58] W. Wang,[71] W. P. Wang,[70,57] X. Wang,[46,g] X. F. Wang,[38,j,k] X. J. Wang,[39] X. L. Wang,[13,f] Y. Wang,[60] Y. D. Wang,[45] Y. F. Wang,[1,57,62] Y. H. Wang,[47] Y. N. Wang,[45] Y. Q. Wang,[1] Yaqian Wang,[17,1] Yi Wang,[60] Z. Wang,[1,57] Z. L. Wang,[71] Z. Y. Wang,[1,62] Ziyi Wang,[62] D. Wei,[69] D. H. Wei,[15] F. Weidner,[67] S. P. Wen,[1] C. W. Wenzel,[4] U. Wiedner,[4] G. Wilkinson,[68] M. Wolke,[74] L. Wollenberg,[4] C. Wu,[39] J. F. Wu,[1,62] L. H. Wu,[1] L. J. Wu,[1,62] X. Wu,[13,f] X. H. Wu,[34] Y. Wu,[70] Y. H. Wu,[54] Y. J. Wu,[31] Z. Wu,[1,57] L. Xia,[70,57] X. M. Xian,[39] T. Xiang,[46,g] D. Xiao,[38,j,k] G. Y. Xiao,[42] S. Y. Xiao,[1] Y. L. Xiao,[13,f] Z. J. Xiao,[41] C. Xie,[42] X. H. Xie,[46,g] Y. Xie,[49] Y. G. Xie,[1,57] Y. H. Xie,[7] Z. P. Xie,[70,57] T. Y. Xing,[1,62] C. F. Xu,[1,62] C. J. Xu,[58] G. F. Xu,[1] H. Y. Xu,[65] Q. J. Xu,[16] Q. N. Xu,[30] W. Xu,[1,62] W. L. Xu,[65] X. P. Xu,[54] Y. C. Xu,[77] Z. P. Xu,[42] Z. S. Xu,[62] F. Yan,[13,f] L. Yan,[13,f] W. B. Yan,[70,57] W. C. Yan,[80] X. Q. Yan,[1] H. J. Yang,[50,e] H. L. Yang,[34] H. X. Yang,[1] Tao Yang,[1] Y. Yang,[13,f] Y. F. Yang,[43] Y. X. Yang,[1,62] Yifan Yang,[1,62] Z. W. Yang,[38,j,k] Z. P. Yao,[49] M. Ye,[1,57] M. H. Ye,[9] J. H. Yin,[1] Z. Y. You,[58] B. X. Yu,[1,57,62] C. X. Yu,[43] G. Yu,[1,62] J. S. Yu,[25,h] T. Yu,[71] X. D. Yu,[46,g] C. Z. Yuan,[1,62] L. Yuan,[2] S. C. Yuan,[1] X. Q. Yuan,[1] Y. Yuan,[1,62] Z. Y. Yuan,[58] C. X. Yue,[39] A. A. Zafar,[72] F. R. Zeng,[49] X. Zeng,[13,f] Y. Zeng,[25,h] Y. J. Zeng,[1,62] X. Y. Zhai,[34] Y. C. Zhai,[49] Y. H. Zhan,[58] A. Q. Zhang,[1,62] B. L. Zhang,[1,62] B. X. Zhang,[1] D. H. Zhang,[43] G. Y. Zhang,[19] H. Zhang,[70] H. H. Zhang,[34] H. H. Zhang,[58] H. Q. Zhang,[1,57,62] H. Y. Zhang,[1,57] J. Zhang,[80] J. J. Zhang,[51] J. L. Zhang,[20] J. Q. Zhang,[41] J. W. Zhang,[1,57,62] J. X. Zhang,[38,j,k] J. Y. Zhang,[1] J. Z. Zhang,[1,62] Jianyu Zhang,[62] Jiawei Zhang,[1,62] L. M. Zhang,[60] L. Q. Zhang,[58] Lei Zhang,[42] P. Zhang,[1,62] Q. Y. Zhang,[39,80] Shuihan Zhang,[1,62] Shulei Zhang,[25,h] X. D. Zhang,[45] X. M. Zhang,[1] X. Y. Zhang,[49] Xuyan Zhang,[54] Y. Zhang,[71] Y. Zhang,[68] Y. T. Zhang,[80] Y. H. Zhang,[1,57] Yan Zhang,[70,57] Yao Zhang,[1] Z. H. Zhang,[1] Z. L. Zhang,[34] Z. Y. Zhang,[43] Z. Y. Zhang,[75] G. Zhao,[1] J. Zhao,[39] J. Y. Zhao,[1,62] J. Z. Zhao,[1,57] Lei Zhao,[70,57] Ling Zhao,[1] M. G. Zhao,[43] S. J. Zhao,[80] Y. B. Zhao,[1,57] Y. X. Zhao,[31,62] Z. G. Zhao,[70,57] A. Zhemchugov,[36,a] B. Zheng,[71] J. P. Zheng,[1,57] W. J. Zheng,[1,62] Y. H. Zheng,[62] B. Zhong,[41] X. Zhong,[58] H. Zhou,[49] L. P. Zhou,[1,62] X. Zhou,[75] X. K. Zhou,[7] X. R. Zhou,[70,57] X. Y. Zhou,[39] Y. Z. Zhou,[13,f] J. Zhu,[43] K. Zhu,[1] K. J. Zhu,[1,57,62] L. Zhu,[34] L. X. Zhu,[62] S. H. Zhu,[69] S. Q. Zhu,[42] T. J. Zhu,[13,f] W. J. Zhu,[13,f] Y. C. Zhu,[70,57] Z. A. Zhu,[1,62] J. H. Zou,[1] and J. Zu[70,57]

(BESIII Collaboration)

[1]*Institute of High Energy Physics, Beijing 100049, People's Republic of China*
[2]*Beihang University, Beijing 100191, People's Republic of China*
[3]*Beijing Institute of Petrochemical Technology, Beijing 102617, People's Republic of China*
[4]*Bochum Ruhr-University, D-44780 Bochum, Germany*
[5]*Budker Institute of Nuclear Physics SB RAS (BINP), Novosibirsk 630090, Russia*
[6]*Carnegie Mellon University, Pittsburgh, Pennsylvania 15213, USA*
[7]*Central China Normal University, Wuhan 430079, People's Republic of China*
[8]*Central South University, Changsha 410083, People's Republic of China*
[9]*China Center of Advanced Science and Technology, Beijing 100190, People's Republic of China*
[10]*China University of Geosciences, Wuhan 430074, People's Republic of China*
[11]*Chung-Ang University, Seoul, 06974, Republic of Korea*
[12]*COMSATS University Islamabad, Lahore Campus, Defence Road, Off Raiwind Road, 54000 Lahore, Pakistan*
[13]*Fudan University, Shanghai 200433, People's Republic of China*
[14]*GSI Helmholtzcentre for Heavy Ion Research GmbH, D-64291 Darmstadt, Germany*
[15]*Guangxi Normal University, Guilin 541004, People's Republic of China*
[16]*Hangzhou Normal University, Hangzhou 310036, People's Republic of China*
[17]*Hebei University, Baoding 071002, People's Republic of China*
[18]*Helmholtz Institute Mainz, Staudinger Weg 18, D-55099 Mainz, Germany*
[19]*Henan Normal University, Xinxiang 453007, People's Republic of China*
[20]*Henan University, Kaifeng 475004, People's Republic of China*
[21]*Henan University of Science and Technology, Luoyang 471003, People's Republic of China*
[22]*Henan University of Technology, Zhengzhou 450001, People's Republic of China*
[23]*Huangshan College, Huangshan 245000, People's Republic of China*
[24]*Hunan Normal University, Changsha 410081, People's Republic of China*
[25]*Hunan University, Changsha 410082, People's Republic of China*
[26]*Indian Institute of Technology Madras, Chennai 600036, India*
[27]*Indiana University, Bloomington, Indiana 47405, USA*
[28a]*INFN Laboratori Nazionali di Frascati, I-00044, Frascati, Italy*
[28b]*INFN Sezione di Perugia, I-06100, Perugia, Italy*
[28c]*University of Perugia, I-06100, Perugia, Italy*
[29a]*INFN Sezione di Ferrara, I-44122, Ferrara, Italy*
[29b]*University of Ferrara, I-44122, Ferrara, Italy*
[30]*Inner Mongolia University, Hohhot 010021, People's Republic of China*
[31]*Institute of Modern Physics, Lanzhou 730000, People's Republic of China*
[32]*Institute of Physics and Technology, Peace Avenue 54B, Ulaanbaatar 13330, Mongolia*
[33]*Instituto de Alta Investigación, Universidad de Tarapacá, Casilla 7D, Arica 1000000, Chile*
[34]*Jilin University, Changchun 130012, People's Republic of China*
[35]*Johannes Gutenberg University of Mainz, Johann-Joachim-Becher-Weg 45, D-55099 Mainz, Germany*
[36]*Joint Institute for Nuclear Research, 141980 Dubna, Moscow region, Russia*
[37]*Justus-Liebig-Universitaet Giessen, II. Physikalisches Institut, Heinrich-Buff-Ring 16, D-35392 Giessen, Germany*
[38]*Lanzhou University, Lanzhou 730000, People's Republic of China*
[39]*Liaoning Normal University, Dalian 116029, People's Republic of China*
[40]*Liaoning University, Shenyang 110036, People's Republic of China*
[41]*Nanjing Normal University, Nanjing 210023, People's Republic of China*
[42]*Nanjing University, Nanjing 210093, People's Republic of China*
[43]*Nankai University, Tianjin 300071, People's Republic of China*
[44]*National Centre for Nuclear Research, Warsaw 02-093, Poland*
[45]*North China Electric Power University, Beijing 102206, People's Republic of China*
[46]*Peking University, Beijing 100871, People's Republic of China*
[47]*Qufu Normal University, Qufu 273165, People's Republic of China*

[48]*Shandong Normal University, Jinan 250014, People's Republic of China*
[49]*Shandong University, Jinan 250100, People's Republic of China*
[50]*Shanghai Jiao Tong University, Shanghai 200240, People's Republic of China*
[51]*Shanxi Normal University, Linfen 041004, People's Republic of China*
[52]*Shanxi University, Taiyuan 030006, People's Republic of China*
[53]*Sichuan University, Chengdu 610064, People's Republic of China*
[54]*Soochow University, Suzhou 215006, People's Republic of China*
[55]*South China Normal University, Guangzhou 510006, People's Republic of China*
[56]*Southeast University, Nanjing 211100, People's Republic of China*
[57]*State Key Laboratory of Particle Detection and Electronics, Beijing 100049, Hefei 230026, People's Republic of China*
[58]*Sun Yat-Sen University, Guangzhou 510275, People's Republic of China*
[59]*Suranaree University of Technology, University Avenue 111, Nakhon Ratchasima 30000, Thailand*
[60]*Tsinghua University, Beijing 100084, People's Republic of China*
[61a]*Turkish Accelerator Center Particle Factory Group, Istinye University, 34010, Istanbul, Turkey*
[61b]*Near East University, Nicosia, North Cyprus, 99138, Mersin 10, Turkey*
[62]*University of Chinese Academy of Sciences, Beijing 100049, People's Republic of China*
[63]*University of Groningen, NL-9747 AA Groningen, The Netherlands*
[64]*University of Hawaii, Honolulu, Hawaii 96822, USA*
[65]*University of Jinan, Jinan 250022, People's Republic of China*
[66]*University of Manchester, Oxford Road, Manchester, M13 9PL, United Kingdom*
[67]*University of Muenster, Wilhelm-Klemm-Strasse 9, 48149 Muenster, Germany*
[68]*University of Oxford, Keble Road, Oxford OX13RH, United Kingdom*
[69]*University of Science and Technology Liaoning, Anshan 114051, People's Republic of China*
[70]*University of Science and Technology of China, Hefei 230026, People's Republic of China*
[71]*University of South China, Hengyang 421001, People's Republic of China*
[72]*University of the Punjab, Lahore-54590, Pakistan*
[73a]*University of Turin and INFN, University of Turin, I-10125, Turin, Italy*
[73b]*University of Eastern Piedmont, I-15121, Alessandria, Italy*
[73c]*INFN, I-10125, Turin, Italy*
[74]*Uppsala University, Box 516, SE-75120 Uppsala, Sweden*
[75]*Wuhan University, Wuhan 430072, People's Republic of China*
[76]*Xinyang Normal University, Xinyang 464000, People's Republic of China*
[77]*Yantai University, Yantai 264005, People's Republic of China*
[78]*Yunnan University, Kunming 650500, People's Republic of China*
[79]*Zhejiang University, Hangzhou 310027, People's Republic of China*
[80]*Zhengzhou University, Zhengzhou 450001, People's Republic of China*

[a] Also at the Moscow Institute of Physics and Technology, Moscow 141700, Russia.
[b] Also at the Novosibirsk State University, Novosibirsk, 630090, Russia.
[c] Also at the NRC "Kurchatov Institute", PNPI, 188300, Gatchina, Russia.
[d] Also at Goethe University Frankfurt, 60323 Frankfurt am Main, Germany.
[e] Also at Key Laboratory for Particle Physics, Astrophysics and Cosmology, Ministry of Education; Shanghai Key Laboratory for Particle Physics and Cosmology; Institute of Nuclear and Particle Physics, Shanghai 200240, People's Republic of China.
[f] Also at Key Laboratory of Nuclear Physics and Ion-beam Application (MOE) and Institute of Modern Physics, Fudan University, Shanghai 200443, People's Republic of China.
[g] Also at State Key Laboratory of Nuclear Physics and Technology, Peking University, Beijing 100871, People's Republic of China.
[h] Also at School of Physics and Electronics, Hunan University, Changsha 410082, China.
[i] Also at Guangdong Provincial Key Laboratory of Nuclear Science, Institute of Quantum Matter, South China Normal University, Guangzhou 510006, China.
[j] Also at Frontiers Science Center for Rare Isotopes, Lanzhou University, Lanzhou 730000, People's Republic of China.
[k] Also at Lanzhou Center for Theoretical Physics, Lanzhou University, Lanzhou 730000, People's Republic of China.
[l] Also at the Department of Mathematical Sciences, IBA, Karachi 75270, Pakistan.